Residual Stress Dependency on Wafer Location of Thin Film PECVD Silicon Nitride

Jeremy R. Godin*, Seong-hoon P. Won* Patricia M. Nieva*, Linh Ngo Phong**, Tim Pope***

*University of Waterloo, Waterloo, ON, Canada, jrgodin@uwaterloo.ca,
**Canadian Space Agency, Saint-Hubert, QC, Canada, linh.ngophong@asc-csa.gc.ca
***INO, Québec, QC, Canada, timothy.pope@ino.ca

ABSTRACT

In this paper we investigate the variations of in-plane residual stress of thin film PEVCD silicon nitride with respect to the local position on a quarter of a 6 inch wafer. Stress measurements are obtained using in-situ fabricated bent beam strain gauges. The deflections of the strain gauges were analytically modelled using an analytical method to correlate them to the stress values. The results of the analytical model were verified using a finite element method (FEM) model and found to be within 1.72 % agreement. The stress measurements obtained using the strain gauges are compared to pre-release stress measurements obtained using a wafer-bow technique. Stress values are reported uniformly at 0 ± 10 MPa before plasma release while post release measurements taken using the strain gauges report an average stress of 69.04 MPa tensile with a standard deviation of 61.47 MPa over the surface of the wafer quarter. Trends in local position values of stress are also observed.

Keywords: silicon nitride, residual stress, local position, bent beam strain gauge, thin film.

1 INTRODUCTION

The construction of free-standing microstructures is one of the fundamental challenges of Micro Electro Mechanical Systems (MEMS) [**1**]. Residual stresses inherent to the deposition process can have profound effects on the functionality and reliability of MEMS devices [**2**]. Internal mechanical stresses cause the free-standing microstructures to warp; buckle up, bent down and ultimately touch down onto the supporting substrate, thus deteriorating the performance of the microsystem or even causing complete failure [**3**]. In addition, the multilayer nature of most MEMS devices causes additional residual stress due to the deposition of different thin film materials and mismatch of their coefficients of thermal expansion (CTE). Beyond deposition, it has been demonstrated that further fabrication steps, such as etching and releasing, are additional sources of residual stress [**4**]. Attempts to control residual stress using different fabrication techniques have been successful in creating PECVD silicon nitride micro devices with relatively low stress values [**5**][**6**][**7**]. However, development of optical microstructures such as microbolometers needs nanometer scale control of thin-film shape, thus greater control of residual stresses [**7**]. Hence, a suitably accurate and efficient method for residual stress analysis is required.

In this paper, we use bent beam strain gauges to measure the the variation on stress distributed across the wafer of a 533 nm thick PECVD silicon nitride film deposited on silicon is studied using bent-beam strain gauges similar to the ones presented in [**8**], [**9**] and shown in Figure 1. Bent beam strain gauges were distributed over the entire surface of a 6 inch wafer. The wafer was cut into quarters after RIE etching and each wafer quarter was released separately at different temperatures and exposure times. This work investigates the stress distribution across a single wafer quarter on after the releasing step. The investigation of the aspects of release parameters such as temperature and release duration and is beyond the scope of this work.

In section 2 the deflections of the strain gauges are modelled using the analytical method described in [**8**] to correlate them to the stress values. Results of the analytical model are then verified with a FEM. In section 3 Measurements of residual stress calculated prior to the patterning and release of the bent-beam strain gauges using the wafer bowing technique are also reported and compared with strain gauge results. Finally, conclusions are made on the variations of stress over the wafer quarter

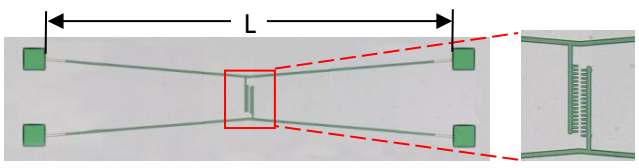

Figure 1: Optical image of a typical bent beam strain gauge which was distributed over the wafer surface. This particular sensor has 0.25 μm Vernier resolution.

2 STRESS ANALYSIS USING BENT BEAM MODELING

The bent beam strain gauge is symmetric along two planes, as such the free body diagram representing a single arm of the structure is presented in Figure 2. The measure of the deflection in the y-axis is read on the Vernier scale at point B, (the apex of the structure), and is used to determine the residual in-plane stress of the film. F is the force required to deform the arm at point B. M_a is the moment acting about the anchor located at the anchor, M is the moment is the arm at any position x, L_a is the actual length of the arm (half the overall device length), L_p is the projected length of the arm onto the x-axis, Δy is the displacement of the apex of the structure and corresponds to half of the Vernier reading, and θ is the angle that the arm makes with the x-axis before release.

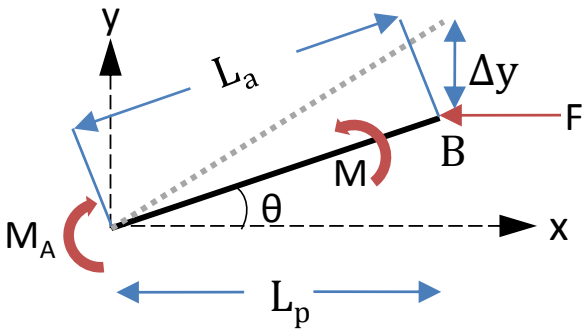

Figure 2: Free body diagram of a half of a bent beam and the forces acting on it [**8**].

The moment equation for the half of the bent beam is[**8**]

$$M = EI\frac{\partial^2 y}{\partial x^2} = M_A - Fy, \tag{1}$$

where M is the moment, E is Young's modulus of the PECVD silicon nitride equal to 125 GPa [**10**], and I is moment of inertia. Since the Vernier gauge is attached to the center of the bent beam, we calculate the stress induced displacement at point B. Eq. (1) has two solutions depending on the sign of force F. In case F is positive (compressive stress), the apex of the bent beams approach each other, and the deflection in the y-axis at B becomes

$$y(F) = \frac{\tan\theta}{\sqrt{F/EI}}\tan\frac{x\sqrt{F/EI}}{4}. \tag{2}$$

Under tensile stress, $y(F)$ becomes

$$y(F) = \frac{\tan\theta}{\sqrt{F/EI}}\tanh\frac{x\sqrt{F/EI}}{4}. \tag{3}$$

The Vernier reading, is the strain of the two bent beams, which can be expressed as

$$2\Delta y = 2[y(F) - y(0)], \tag{4}$$

where $y(0)$ is y value when the force is zero (F=0). By varying the force value, Vernier readings can be calculated along with the corresponding in-plane stress. The stress (δ) is expressed as:

$$\delta = E\frac{\Delta L}{x} + \frac{F}{wh}, \tag{5}$$

$$\Delta L' = \big(L_a(0) - L_p(0)\big) - \big(L_a(F) - L_p(F)\big) \tag{6}$$

where $\Delta L'$ is the change of the length difference between the actual beam and its projected length on x-axis due to force F, w is width of the beam, and h is the height of the beam. The difference between the elongated length of the beam and its projected length along the x-axis (L') of the half of the bent beam is [**11**]

$$L'(F)/2 = -\frac{1}{2}\int_0^{L/2}\frac{\partial y(F)}{\partial x}dx. \tag{7}$$

The length change due to a tension force ($F > 0$) is:

$$\begin{aligned}\Delta L' &= L'(F) - L'(0)\\ &= \frac{(\tan\theta)^2}{4k}[2H + kx - kxH^2 + \sinh(kx)\\ &\quad - 2H\cosh(kx) + H^2\sinh(kx)] - L'(0).\end{aligned} \tag{8}$$

For a compression force, ($F < 0$) length change is

$$\begin{aligned}\Delta L' = L'(F) - L'(0) = \frac{(\tan\theta)^2}{4k}[2G + kx + kxG^2\\ + \sin(kx) - 2G\cos(kx) - G^2\sin(kx)] - L'(0),\end{aligned} \tag{9}$$

where $k = \sqrt{F/EI}$, $H = \tan(kx/4)$ and $G = \tanh(kx/4)$. By varying the force F, in equations (4) and (5), a curve was generated in Figure 3 relating the Vernier reading and its corresponding stress value.

The bent beam strain gauge analytical model was compared against an ANSYS™ simulation for validation, also shown in Figure 3. The simulation was conducted using the 3D 20-Node Structural Solid element SOLID186. The bent beam strain gauges were simplified to a single bent deflection beam anchored at both ends. Residual stress was implemented into the model using the pre-stress command, whereby the stress in the x and y directions where set. To acquire the FEM Vernier reading stress curve of Figure 3, the simulation was run for initial stress values ranging from −170 MPa (compressive) to 170 MPa (tensile) in steps of 10 MPa and the deflections were plotted in excel.

The Vernier reading stress curves for both the analytical and FEM models were fitted to a 3rd order polynomial in excel (Figure 3). Analyses of the fitted curves for both methods show nearly linear curves in the calculated regimes, which agrees with the results presented in [**9**] and [**8**]. The linear coefficient is the overwhelmingly dominating term in both fitted curves and differs by only 1.72%. This small difference corresponds to a maximum difference in

predicted stress values of 0.716% (1.18MPa tensile) and 2.67% (4.65MPa compressive) in the calculated range of Vernier reading from -5 µm to 5 µm tensile.

Since the analytical model is consistent with the FEM model, it is assumed that the analytical solution is valid. Therefore, we use the analytical model to calculate the stress measured by the bent beam strain gauges.

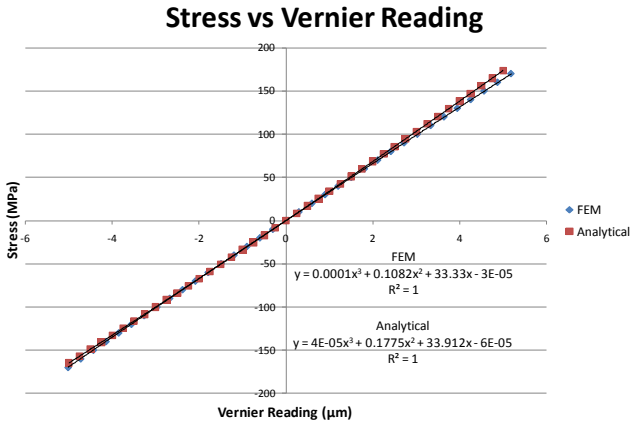

Figure 3: Modeling of residual stress and deflection of a bent beam strain gauge using the analytical and the FEM models. Positive values indicate tensile stress.

3 RESIDUAL STRESS ANALYSIS OF SILICON NITRIDE THIN FILMS

The bent beam strain gauge design for this paper was fabricated from a 1-mask process of PECVD silicon nitride deposited with a thickness of 533 nm. The wafer was organized into chips 5 mm by 5 mm and the bent beams were placed onto a large number of the chips evenly distributed over the surface. As discussed previously, the stress values of only a single wafer quarter are present in this paper.

As shown in Figure 1, the Vernier readings of the bent beams were measured using a standard optical microscope at a perpendicular angle to the wafer surface in order to eliminate parallax error. However, the stress gradient within the PECVD silicon nitride layer caused the suspended Vernier structure to bend downwards and "stick" to the silicon substrate surface. It was assumed that the effect of stiction had no effect on the reading of the Vernier gauge since stiction would have occurred after the in plane deflection of the bent beam, thus not affecting the actual measurement.

A surface plot of the measured residual stress of the quarter wafer is shown in Figure 4. The surface was constructed in MATLAB using a bicubic interpolation of the recorded stress values of each device, depicted by the blue points on the surface. The projected shaped of the wafer quarter is outlined in red below the surface plot. From the plot we see a large variation in residual stress over the surface. The average stress on the wafer reported using the bent beam strain gauges is 69.04 MPa with a standard deviation of 61.47 MPa, and maximum and minimum stresses of −82.65 MPa compressive and 143.61 MPa tensile respectively.

Wafer bow measurements were conducted on the full wafer after the deposition of 533 nm of PECVD silicon nitride, but before reactive ion etching (RIE) of the layer. The results from the wafer bow measurements characterized the stress of the entire wafer after deposition as 0 ± 10 MPa. It is our belief that the increase in residual stress is due primarily to the releasing process. While the RIE etching can also be responsible for the increase in stress, it is our belief that the high temperature and exposure time of the plasma release is a more likely candidate for the stress. However, further experimentation is required to conclude this hypothesis and is part of our ongoing research.

Figure 5 depicts the residual stress dependence on radial distance from the center of the wafer (row 19 and column 19). We can observe that at the center of the wafer, the residual stresses are tensile with an average value of about −100 MPa. However, as the radial distance increases from the center towards the edge of the wafer, the stresses become increasingly more compressive with an average value of about −100 MPa. This phenomenon can be related to what it is known as "*film edge-induced stress*", and has been extensively studied in the field of silicon microfabrication technology for the case of complete wafers [**12**]. In this case, a discontinuity (edge) of a surface film gives rise to an edge force which brings about a partial relaxation in the film and reduces the stress. For our particular case, the large variation of stress observed (from +100 MPa at the center to −100 MPa at the edge of the wafer) is attributed to this film edge-induced stress.

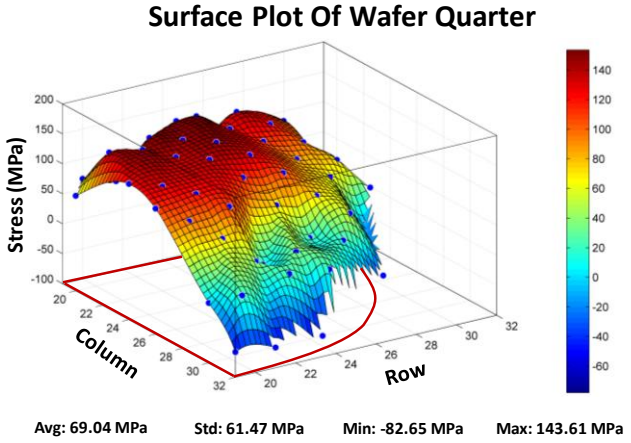

Figure 4: Bicubic interpolation surface plot of in-place residual stress of a wafer quarter with a 533 nm thick PECVD silicon nitride film. The blue dots are the measured values of stress. Tensile stress is positive.

Observation of the surface plots in Figure 4 and the radial plot in Figure 5 also show that there is a distinct drop in residual stress from the center of the wafer quarter

(approximately chip row 26, column 26) to its boundaries. We believe that the reduction in tensile stress at the diced edges is also indicative of film edge-induced stress but compared to the effect of this stress at the wafer edge, it is less pronounced. An explanation to this could be that since dicing of the wafer took place after the deposition process and unlike the case of the wafer edge, no film edge-induced stress was present before releasing.

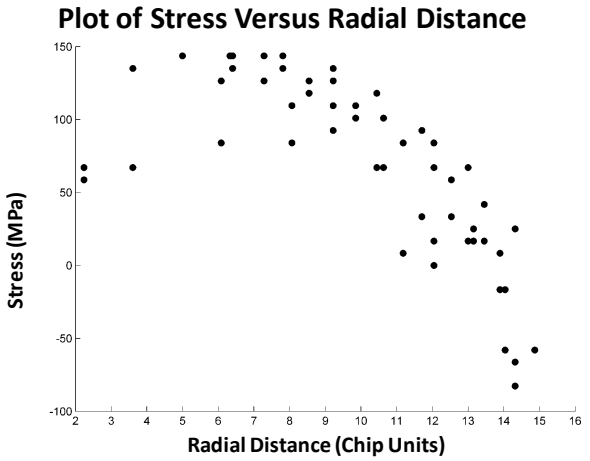

Figure 5: In-plane residual stress distribution as a function of radial distance from the center of the wafer. Tensile stress is positive.

4 CONCLUSION AND FUTURE WORK

We have shown the feasibility of using bent beam strain gauges for the local position measurement of in-plane stress in PECVD silicon nitride thin films.

In this paper we revisited the analytical model of bent beam strain sensors as presented in [**8**], and validated the results using an FEM model. Both models produced nearly linear relationships between deflection of the device and applied residual stress based on fitted curves. The dominant linear coefficients of each curve were in close agreement, differing by only 1.72 %. The maximum difference in predicted residual stress between the models was found to be 1.18 MPa (tensile) and 4.65 MPa (compressive), over the range of stresses investigated. Wafer bow measurements of the wafer were conducted prior to RIE etching measuring the stress at 0 ± 10 MPa. The large difference in wafer bow and bent beam strain gauge measurements is thought to be induced during the plasma releasing stage of fabrication; ongoing studies are being done to further investigate this problem.

Using bent beam strain gauges, the residual stress in a quarter of a wafer was reported. An average stress of 69.04 MPa was measured with a standard deviation of 61.47 MPa indicating a large gradient in stress values over the wafer surface. Variations in local stress values were investigated, using radial distance plots. Further work will investigate the possible causes of variations in local stress.

5 ACKNOWLEDGEMENTS

Funding for this work was provided by CSA under contract #64-7009003. The devices were fabricated onsite at INO Quebec. The authors would also like to acknowledge the contribution of Bruno Fisette from INO for the fabrication assistance he provided.

REFERENCES

[1] K J Winchester and J M Dell, "Tunable Fabry-Perot cavities fabricated from PECVD silicon nitride," *J. Micromech. & Microeng.*, pp. 589-594, 2001.

[2] E.M. Ochoa, J.A. Lott, M.S. Amer, W.D. Cowan and J.D. Busbee L.A. Starman_Jr., "Residual Stress Characterization in MEMS Microbridges," *Sensors and Actuators A*, vol. 104, no. 2, 2002.

[3] E Cianci, A Coppa, and V Foglietti, "Young's modulus and residual stress of DF PECVD silicon nitride," *Microelec. eng.*, pp. 1296-1299, 2007.

[4] Mary Vechery, Andrew Dick, B Balachandran, and Madan Dubey, "Pre and Post machining and release residual stresses," in *Nanosensors and Microsensors for Bio-Systems*, San Diego, CA, United states, 2008.

[5] M Martyniuk, J Antoszewski, C A Musca, J M Dell, and L Faraone, "Stress in low-temperature PECVD silicon nitride thin films," *Smart Mat. & Struct.*, pp. S29-S38, 2006.

[6] A Tarraf, J Daleiden, S Irmer, D Prasai, and H Hillmer, "Stress investigation of PECVD dielectric layers for advanced optical MEMS," *J. MEMS*, pp. 317-323, 2004.

[7] Thomas G Bifano, Harley T Johnson, Paul Bierden, and Raji Krishnamoorthy Mali, "Elimination of Stress-Induced Curvature in Thin-Film Structures," *J. MEMS*, pp. 592-597, 2002.

[8] Yogesh B Gianchandani and Khalil Najafi, "Bent-Beam Strain Sensors," *J. MEMS*, pp. 52-58, 1996.

[9] Matthew R Begley and N Scott Barker, "Analysis and design of kinked beam sensors," *J. Micromech. & Microeng.*, pp. 350-357, 2007.

[10] M W Denhoff, "A measurement of Young's Modulus and residual stress in MEMS bridges using a surface profilometer," *J. Micromech. & Microeng.*, vol. 13, pp. 686-692, 2003.

[11] Raymond J. Roark and Warren C. Young, *Formulars for stress and strain*, 5th ed. New York, USA: McGraw-Hill Book Company, 1975.

[12] A Atkison, T Johnson, A H Harker, and S C Jain, "Film edge-induced stress in substrates and finite films," *Thin Solid Films*, vol. 274, pp. 106-112, August 1996.